Article

Assessment of Sediment Impact on the Risk of River Diversion during Dam Construction: A Simulation-Based Project Study on the Jing River, China

Zida Song [1], Quan Liu [1,*] [iD], Zhigen Hu [1], Huian Li [2] and Jianqing Xiong [2]

1   State Key Laboratory of Water Resources & Hydropower Engineering Science, Wuhan University, Wuhan 430072, China; zidasong@163.com (Z.S.); zhigenhu@163.com (Z.H.)
2   Yellow River Engineering Consulting Co., Ltd., Zhengzhou 450003, China; liha@yrec.cn (H.L.); xiongjq@yrec.cn (J.X.)
*   Correspondence: hapland@whu.edu.cn; Tel.: +86-130-7127-9891

Abstract: Dams are vital for water resource utilization, and river diversion is key for dam construction safety. As sandy river basins are important exploitation areas that have special diversion features, the impact of sediment on the risk of river diversion during dam construction should be assessed. Diversion uncertainty is the origin of diversion risk, and sediment uncertainty changes the storage and discharge patterns of the diversion system. Two Gumbel–Hougaard (GH) copula functions are adopted to couple the random variables of flood and sediment, so that the sediment impacts on diversion storage and discharge can be obtained by the sampling of flood peaks. Based on variable coupling and sediment amendment, a method of Monte Carlo simulation (MCS) with a water balance calculation can quantitatively assess the risk of sandy river diversion, by evaluating the probability of upstream cofferdam overtopping. By introducing one diversion project on the Jing River in China with a clear water contrast, the risk values of dam construction diversion with or without sediment impacts can be obtained. Results show that the MCS method is feasible for diversion risk assessment; sediment has a negative impact on the risk of river diversion during dam construction, and this degradation effect is more evident for high-assurance diversion schemes.

Keywords: risk assessment; river diversion during dam construction; sediment uncertainty; GH-copula function; Monte-Carlo simulation; Jing River

1. Introduction

Water dams are one of the most important and feasible tools for water resource management and utilization. Applied to rivers worldwide, the purposes of dams include irrigation, hydropower, water supply, and flood control [1]. Moreover, water demand is steadily growing [1,2] and hydroelectricity still has great potential as one vital part of renewable energy [3] in China, the rest of Asia, Africa, and Latin America, so far [4–6]. Hence, the growth of human population and the development of economies keep prompting a global boom in dam construction [7]. Predictably, many regions worldwide (especially developing countries) will confront the construction of water dams within decades, and construction locations include general clear water rivers and sandy rivers with sediment impact. However, with massive volumes of reservoir water and a vast range of influence, dam failures may lead to serious socioeconomic losses, and many catastrophic failure cases happened in the course of construction [8]. When dam construction projects fail during the process, huge financial losses, flooding, and even human casualties may occur, and the aftermath will impair the region's economic

stability and security [9,10]. Consequently, techniques that enhance risk regulation during dam construction are of great significance to global water resource management and can boost confidence in dam construction.

Generally, dams are built in watercourses, therefore interferences from river flow are the main risk source during the construction process. To free the dam foundation pit from river water, certain engineering methods should be applied in advance, i.e., river diversion during dam construction [11–14]. This type of temporary flow control system can partly or completely divert the river, so that a dry riverbed is provided for dam construction. For dam construction diversion modes, the most common one involves a pair of river-cutoff cofferdams and diversion tunnels [14,15]. The typical dam construction diversion layout of this type can be seen in Figure 1. In the figure, the positions of cofferdams, the diversion tunnel, the upstream cofferdam reservoir, and the dry construction pit are shown, and the diverted river flow direction is indicated.
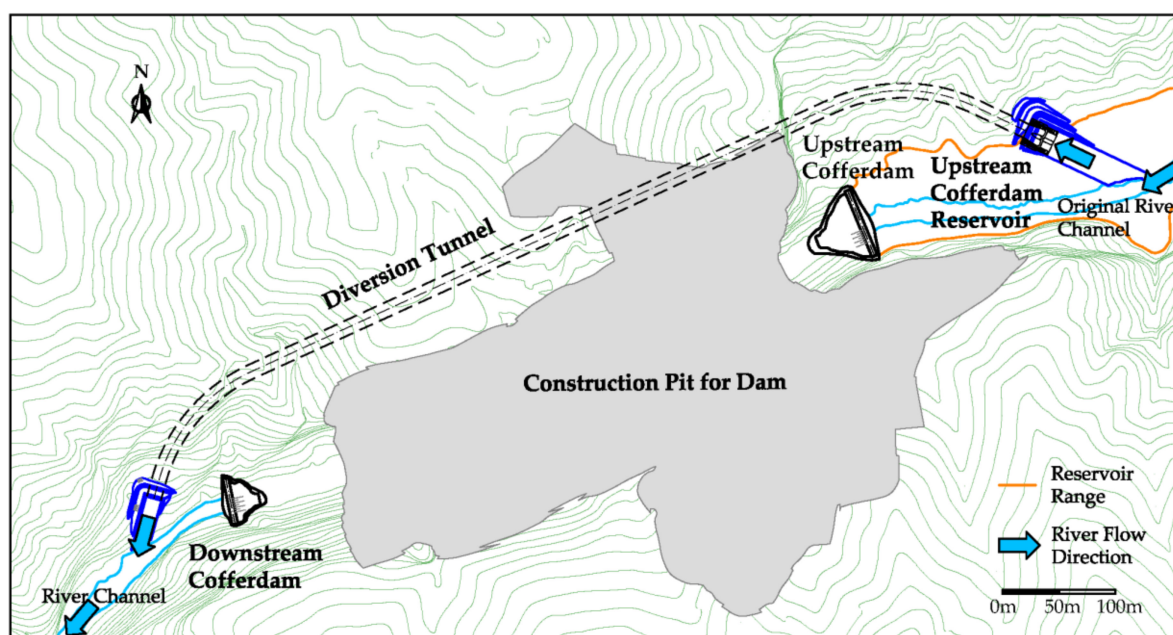

Figure 1. Typical layout of cofferdam and tunnel mode dam construction diversion.

Moreover, as diversion buildings will be abandoned after dam construction, cofferdams are mainly earth–rock structures for cost reasons [10,16]. Hence, for cofferdam and tunnel diversion, when cofferdam overtopping occurs during extreme flood conditions, an earth–rock cofferdam may breach, after which construction pits are submerged, and a series of subsequent impacts are posed on the whole construction project. Obviously, once the flood overtops the upstream cofferdam of a dam construction diversion system, the project can be considered to have suffered a major accident, and such failure constitutes the main risk event of river diversion during dam construction [10,12,14,16].

Present risk-related research about river diversion during dam construction mainly focus on process security and integral economy, which are rooted in actual water resource management demand [9,14]. Furthermore, as risk factors are mainly water-related, uncertainties about hydraulic and hydrologic factors were the main concerns for scholars [12,15,17–19]. Specifically, incoming flood uncertainty and discharge uncertainty affect the degree of risk, as water levels of the upstream cofferdam reservoirs rise and incur overtopping when inflow exceeds outflow in volume [17–19].

The studies above include detailed discussion of the river diversion risk under various dam construction conditions, and the effects that multiple uncertainties impose. Nevertheless, none of them have the impact posed by river sediment on diversion systems currently under consideration. As sandy rivers, like the Yellow River in China and the Nile River in Egypt, are the main sources of

hydropower and agricultural water for those areas, dams will be constructed under sediment impact. These sandy river flows may not be typical Newtonian fluids [20], and similar to floods, sediment possesses uncertainty as well [21–24]. Therefore, sandy rivers generally have different hydraulic features from ordinary rivers [25,26]. Obviously, the risk evaluation of dam construction diversion on sandy rivers is more complicated than in clear water cases. Moreover, when making decisions, a tradeoff between initial investment and construction failure risk during the building process is usually necessary for good dam construction diversion designs [9,15,17,27], and quantitative risk measurement serves as an important decision reference. Hence, comprehensive research to evaluate the impact of sediment on risk evaluation of river diversion during dam construction is highly necessary.

To provide a practical risk assessment method for dam construction diversion on sandy rivers, this paper considers the uncertainties of sediment and flooding, and adopts a simulation technique to evaluate the risk. Detailed explanations of the uncertainties of water and sediment are coupled via Gumbel–Hougaard (GH) copula function; then, incoming flooding, diversion storage, and diversion system discharge volume samples are generated using a Monte–Carlo simulation (MCS). With multiple groups of simulated inflow and outflow data, the probabilistic relation between diversion works overtopping and upstream cofferdam elevation is depicted through the water balance calculation. In this way, the risk of sandy river diversion during dam construction can be assessed in a quantitative manner. Furthermore, based on a hydropower dam project on the Jing River, one of the main sediment-laden rivers in China, and a contrasting clear-water case, the diversion risk variation caused by the impact of sediment can be evaluated through this paper's method. Supported by the risk assessment results and related analysis, the influence on dam construction diversion brought by sediment can be revealed, and the risk features of sandy river diversion can assist with the diversion decision.

2. Study Area

The hydropower project in this study is situated at one section of the Jing River, which is 100 kilometers northwest of Xi'an, a major city in northwest China. The Jing River is one of the main tributaries of the Wei River, and the Wei River is the most important tributary of the Yellow River. A map indicating the study area is shown in Figure 2 (the map is adapted from Kmusser's work [28]). It can be seen from the map that the project site is located in the southeast region of Wei River basin, and is near to the junction of Wei and Jing River.

Figure 2. Location of the study area on the Jing River in the Wei River basin.

As the third-largest river in Asia, the Yellow River is well-known for its high sediment concentration during flood seasons. Having the same feature, the flooding of the Jing River is also hyper-concentrated. For this typical sandy river, data about hydrology and sediment in the Jing River watershed can be obtained from local hydrologic stations. As the data shows, the multi-year average sediment concentration in flood seasons is 212 kg/m^3, the maximum recorded sediment concentration in the field is 1428 kg/m^3, and the multi-year average sediment yield is 2.48×10^8 t. The median particle diameter is 0.021 mm, and the recommend dry bulk density of silt is 1.3 t/m^3. The annual river runoff volume is 1.72 billion m^3. The data indicates that the properties of the Jing River flow are obviously different from that of clear water flow [20], and the high sediment concentration of the Jing River in flood seasons also highlights the differences. As the Jing River is located in the loess plateau of China, the main sediment origin of Jing River is loess, which is very fine and lacks cohesion; in addition, the sediment content of cohesive particles like clay is not high. Therefore, sediment cohesion is not evident for river diversion on the Jing River. Furthermore, by determining the proper deposit rate and diversion discharge coefficient, based on regional hydrology and sediment data, the cohesion of the field river flow can be reflected. Hence, sediment impact should be considered with regards to the diversion project on the Jing River, and key diversion parameters that are related to discharge, like the cofferdam reservoir deposit rate and hydraulic roughness, should be determined by local field-measured data.

This paper's study area is on the Jing River, and the research objective is the risk of river diversion during dam construction. As the risk of dam construction diversion derives from indetermination, diversion uncertainties on the Jing River are the key part of this study, which mainly includes flooding, diversion discharge, and sediment factors.

3. Diversion Uncertainties

As mentioned, for general rivers, hydrologic and hydraulic uncertainties are the main risk factors, which respectively represent the flood and diversion system discharge uncertainties in practice [17–19]. Nevertheless, for sandy rivers, the impact of sediment should also be considered. In the Jing River project case, the uncertainties of flooding, diversion discharge, and sediment together control the inflow, outflow, and cofferdam reservoir capacity of the diversion system. Hence the diversion uncertainties should be analyzed in detail, and appropriate mathematical models can be introduced to describe them. Furthermore, the relationship between these uncertainties can be explored and utilized, which is helpful for the subsequent study.

3.1. Flood Uncertainty

Flooding was the major risk factor in diversion risk studies, and it is evident that flooding possesses uncertainty. This uncertainty is considered as one hydrology-based uncertainty that can be predicted by historical hydrology data, because it obeys certain types of distribution [9,12–18,29]. Here, the Pearson III distribution was selected to describe the flooding uncertainty in the diversion system, as supported by previous literature [29–31] and generally adopted in China [18,19,32]. The probability density function of Pearson III distribution is:

$$f(x) = \frac{\beta^\alpha}{\Gamma(\alpha)}(x - a_0)^{\alpha-1} e^{-\beta(x-a_0)} \tag{1}$$

Here, α, β, and a_0 are the distribution parameters of the Pearson III distribution: $\Gamma(\alpha)$ is the Gamma function of α, and x is the value of the random variable that obeys Pearson III distribution.

$$\alpha = \frac{4}{C_s{}^2}, \ \beta = \frac{2}{xC_vC_s}, \ a_0 = \bar{x}\left(1 - \frac{2C_v}{C_s}\right) \tag{2}$$

Here, C_s, C_v, and $\bar{x}$ are the coefficient of deviation, the coefficient of variation, and the mean value, respectively.

3.2. Diversion System Discharge Uncertainty

Another diversion uncertainty is related to the diversion system itself, i.e., the uncertainty of the flow discharge ability of the diversion buildings [17,18]. Generally, the actual discharge ability of diversion buildings, such as diversion tunnels, is not identical to their designed discharge ability. Therefore, even for the same tunnel, the discharge volume varies under different diversion conditions. As the discharge coefficient of diversion tunnels has great relevance to the value of hydraulic roughness, which is undetermined [29,33,34], the uncertainty of diversion discharge can be correlated to the roughness variability, and this roughness variability appears in the triangular distribution [29,33].

The hydraulic characteristics of sandy river flows relate to river sediment, and are different from that of clear water rivers [20,25]. Therefore, sediment uncertainty should be involved in the calculation of hydraulic roughness on sandy rivers, and the result needs treatment based on triangular distribution. Hence, in this study, when considering sediment impact, the diversion system discharge uncertainty is described by sediment uncertainty, as the diversion discharge coefficient is obtained based on the value of the hydraulic roughness. Meanwhile, the calculation of hydraulic roughness involves sediment uncertainty, and is treated by triangular distribution.

3.3. Sediment Uncertainty

River sediment is a hydrological phenomenon, with uncertainty in timing and amount [23], and it also has a dynamic process of production and transportation. Though complicated, sediment uncertainty can still be described by certain mathematical models, according to some scholars. Lee adopted Pearson III distribution, the same distribution that describes flood uncertainty, to predict the movement of sediment particles [35]. More straightforwardly, in Li's study, Pearson III distribution was used for the frequency analysis of the sequence of sediment discharges during a long period at certain hydrologic station [36], and Jin considered that the middle Yellow River sediment adapted to Pearson III distribution [37]. Considering the fact that river sediment and flooding may share the same origin, since both of them can be triggered by intense rainfall, the Pearson III distribution is appropriate for the description of sediment uncertainty. Furthermore, previous literature proved that a correlation exists between sediment and flooding [38,39]. Hence, in this paper, river sediment and flooding are considered to obey the same distribution, the Pearson III distribution.

Not only related to flooding, river sediment also influences two key factors of the diversion system, i.e., the diversion discharge ability and the cofferdam reservoir capacity. Sediment changes the hydraulic characteristics of river flow, which influences its diversion discharge ability. Meanwhile, sediment-laden flows during flood seasons can cause evident siltation in the upstream cofferdam reservoir, thus reducing the available capacity of the diversion system and weakening the system's flood detention ability [40].

3.4. Sediment Impact on Diversion System

To fully describe the mechanism of sediment impact on diversion systems, details about how to determine the data of reservoir capacity and discharge ability should be explained. Noticeably, this paper only discusses the cofferdam and tunnel diversion mode, and in this section, some of the equations involved are empirical and non-unique.

As river sediment mainly influences the cofferdam reservoir by causing sedimentation, the volume of reservoir sediment deposition should be calculated. Currently, multiple models are proposed to predict the sediment transport: Meyer-Peter and Müller [41], Engelund-Hansen, Yang, Ackers-White, Van Rijin etc. [42,43]. Among the models, the Engelund-Hansen and Van Rijin models are used for the prediction of the suspended load transport rate [43]. The Meyer-Peter and Müller model is widely applied for the calculation of the bed load transport rate [44,45]. In Dysarz's work [46],

the Meyer-Peter and Müller model and Engelund-Hansen model are applied for the calculation of sediment transport, as they reflect the sediment uncertainty and are used for the generation of river bottom profiles. These models are feasible for the prediction of sediment transport rate and have shown good application results on general rivers [44,46]. However, the applicability of these models on hyper-concentrated sandy rivers, like the sediment-laden flow of the Jing River remains unclear, for lack of supportive literatures on application. Moreover, the Meyer-Peter and Müller model is based on laboratory experiments for coarse sediments, like coarse sands and gravel [41,46], but the Jing River has very fine silt, with a median particle diameter of only 0.021 mm. The Van Rijin model has better results than the Engelund-Hansen and Ackers-White models on the lower reach of the Yellow River, near the Bohai Sea Gulf [43]. However, the Jing River is located on the middle reach of the Yellow River, where the river channel is deeper and narrower, and sediment conditions are also quite different from those of the lower reach. Therefore, the sediment transport feature of the Jing River is different from that of the Yellow River lower reach.

Instead of a model-based prediction method, field observation and measurement data from local hydrologic stations and proper sediment uncertainty descriptions are adopted in this paper. As the Jing River has plenty of official hydrologic stations, which can provide reliable hydrology and sediment data over a long period, the field data of sediment transport is the basis for the sediment deposition calculation in this paper. Meantime, as mentioned Section 3.3, sediment is considered as obeying Pearson III distribution in China. Therefore, simulation-based sampling that uses field measured data and obeys Pearson III distribution can generate reliable sediment transport parameters for the Jing River. To estimate the shrink of the cofferdam reservoir capacity, there is an equation commonly used in China [47] to calculate reservoir sediment deposition volume V_s:

$$V_s = (1 + \eta) \frac{\delta W}{(1 - \phi) r_s} T \tag{3}$$

where W is the annual sediment yield, ϕ is the sediment porosity, η is the ratio of the bed load among the suspended load, r_s is the dry bulk density of silt, δ is the deposit rate based on regional hydrology and sediment data, and T is the span of deposition (in years).

Among all the parameters of Formula (3), W is the one that involves sediment uncertainty, and can be determined based on field data from hydrologic stations through simulation-based sampling; meanwhile, ϕ and δ are generally set as 0.3 and 1.18%, based on the field observation. The specific data of η and r_s can be determined by hydrologic observation and field measurement as 0.0008 and 1.3 t/m^3 in Jing River, respectively. T is set as 0.5 years in this paper, considering the cofferdam construction schedule. Only W, the annual sediment yield, involves uncertainty. Hence, W is the independent variable for calculating V_s.

Generally, as seen through measurement and hydrological observation, the relation between origin upstream cofferdam reservoir capacity V and reservoir water level H_u before the completion of cofferdam construction can be obtained. With the known V-H_u relation and sediment deposition volume V_s, the sediment deposition-impacted upstream cofferdam reservoir capacity V' can be determined by Formula (4), which is a function controlled by the annual sediment yield W and reservoir water level H_u. Hence, the V'–H_u relationship is determined by Formula (4).

$$V' = V - V_s = f_1(H_u, W) \tag{4}$$

The impact that sediment poses on a diversion discharge system involves several hydraulic and sediment dynamics elements, and is also closely linked to the sediment concentration.

Under most operation conditions, river water is discharged via diversion tunnels in a pressure flow from upstream to downstream of cofferdams. According to the Chinese design specification [48], the discharge capacity is expressed by Formula (5):

$$q = \mu A \sqrt{2g \left(H_0 + iL - h_p \right)} \tag{5}$$

where q is the quantity of diversion discharge flow, μ is the discharge coefficient of the diversion tunnel, A is the cross-section area of the discharge tunnel, g is the gravitational acceleration, i is the gradient, L is the length of the diversion tunnel, H_0 is the upstream waterhead, and h_p is the difference between the downstream water level and the downstream diversion tunnel exit elevation.

Among all the parameters of Formula (5), the values of A, g, I, and L, as well as the downstream tunnel exit elevation are provided or known according to the design. Downstream water level is determined by H_0 and the relation of channel's natural runoff and water level. H_0 generally adopts the upstream water level in practice. The discharge coefficient μ can be calculated by Formula (6):

$$\mu = \frac{1}{\sqrt{1 + \sum \zeta + \frac{2gL}{C_d^2 R_d}}} \tag{6}$$

where $\sum \zeta$ is the sum of waterhead loss, C_d is the Chézy coefficient, and R_d is the hydraulic radius.

Variables $\sum \zeta$ and R_d can be measured according to the design and the shape of diversion tunnels, and C_d can be determined through Manning's derivation [49]:

$$C_d = \frac{1}{n} R_d^{1/6} \tag{7}$$

where n is the synthesis roughness coefficient of the diversion tunnel.

For a sediment-laden flow, the sediment concentration influences roughness coefficient n through the Karman constant κ [50,51]. According to Deng's study [51] and the triangular distribution treatment requirement for diversion tunnels, the $n - \kappa$ relationship is described by Formula (8):

$$\begin{cases} n^* = \frac{\kappa R_d^{1/6}}{7.2 \log(12.2 \frac{R_d \chi}{k_s})} \\ n = Tri(n^*) \end{cases} \tag{8}$$

where n^* is the value of calculated roughness that only considers sediment influence, according to Deng's study [51]; χ is the correction coefficient, generally set as 1; k_s is the side wall protrusion height, and is set as 0.02 m in this paper; $Tri()$ is the triangular distribution treatment function, and its triangular distribution parameters of maximum, median, and minimum are set as 0.98, 1.00, 1.02, respectively.

Based on the mass observation data of sediment-laden flows in China, Karman constant κ can be calculated by Formula (9) [52]:

$$\kappa = 0.4 - 1.68 \sqrt{S_v} (0.365 - S_v) \tag{9}$$

Here, S_v is the volume sediment concentration, $S_v = S/r_s$, r_s is the dry bulk density of silt, and S is the flow average sediment concentration in flood seasons.

Hence, based on Formulas (6)–(9), with the average sediment concentration in flood seasons S and all the known parameters, the roughness coefficient n can be derived from S with the triangular distribution treatment, after which the discharge coefficient μ can be obtained. S involves sediment uncertainty, and can be determined through simulation-based sampling.

By combining Formula (5) and roughness coefficient n-based discharge coefficient μ, the sediment impacted discharge ability q' can be determined with the upstream waterhead H_0, which is generally set as the water level at upstream cofferdam.

Hence, Formulas (5)–(9) constitute the determination function of the sediment-impacted diversion discharge ability q'. H_0 and n (based on S) are the independent variables of the q' determination function:

$$q' = f_2(H_0, n) \tag{10}$$

3.5. Coupling of Flood and Sediment Uncertainties

As mentioned, flooding and sediment are random variables with correlation, and the sediment uncertainty influences the cofferdam reservoir capacity, and reflects discharge ability of the diversion system. Hence, by utilizing the correlation between flood and sediment, the uncertainties of flood, sediment, and discharge can be strung together, which facilitates the simulation of uncertainties.

Evidently, a water and sediment joint distribution should be developed to indicate the correlation between a flood and sediment. As is commonly applied in the hydraulic field [53–55], the theory of the Gumbel–Hougaard (GH) copula function [56] is introduced for coupling the flood and sediment variables. Expression (11) can reflect the marginal distribution characteristics of the peak flood volume towards the sediment parameter, and describe the nonlinear relationship between flooding and sediment.

$$\begin{cases} F(y,z) = \exp\left\{ -\left[(-\ln u)^{\theta} + (-\ln v)^{\theta} \right]^{1/\theta} \right\} \\ u = F_Y(y) \\ v = F_Z(z) \end{cases} \tag{11}$$

Here, $F_Y(y)$ is the marginal distribution function of flood peak variable y, complying with Pearson III distribution. $F_Z(z)$ is the marginal distribution function of sediment variables z (including the variable of annual sediment yield as well as average sediment concentration in flood seasons), all complying with the Pearson III distribution. θ is controlled by τ as $1/\theta = 1 - \tau$, and τ is the Kendall correlation coefficient, which describes the nonlinear relationship among variables and is obtained by Formula (12):

$$\tau = \frac{1}{C_k^2} \sum_{i<j} sign\left[(y_i - y_j)(z_i - z_j) \right] \tag{12}$$

where C_k^2 is the combinatorial number of two variables with a length of k, (y_i, z_i) is the sample data of flood peak and sediment variables, and $sign(\cdot)$ is the sign function.

As is described in Formulas (4) and (10), the reservoir capacity is amended based on annual sediment yield W, and the discharge ability is amended based on the average sediment concentration in flood seasons S through hydraulic roughness n. Therefore, two separate GH copula functions of "flood peak–annual sediment yield" and "flood peak–average sediment concentration in flood seasons" should be established. In these functions, p will represent a sample value of flood peak volume, w will represent the corresponding sample value of annual sediment yield W, and s will represent the corresponding sample value of the average sediment concentration of flood S. Then, based on Formula (11), the uncertainties of flood and sediment can be coupled. The two GH copula functions of "flood peak–annual sediment yield" and "flood peak–average sediment concentration in flood seasons" are shown in Formulas (13) and (14).

$$F_{QW}(p,w) = \exp\left\{ -\left[(-\ln F_Q(p))^{\theta_1} + (-\ln F_W(w))^{\theta_1} \right]^{1/\theta_1} \right\} \tag{13}$$

$$F_{QS}(p,s) = \exp\left\{ -\left[(-\ln F_Q(p))^{\theta_2} + (-\ln F_S(s))^{\theta_2} \right]^{1/\theta_2} \right\} \tag{14}$$

Here, $F_Q(p)$, $F_W(w)$, $F_S(s)$ are the marginal distribution functions of flood peak, annual sediment yield, and average sediment concentration in flood seasons, respectively. All three functions complying with Pearson III distribution.

With the two GH copula functions, only by inputting the sample of flood peak *p* can the corresponding sample values of *s* and *w* be generated. In practice, the appropriate sample of flood peak *p* can be generated through simulation based on hydrologic data of the watershed and the Pearson III distribution in Formula (1).

To facilitate the comprehension of the relationships among diversion uncertainties, an indication sketch is provided based on Section 3. The relationships among the diversion uncertainties can be seen in Figure 3.
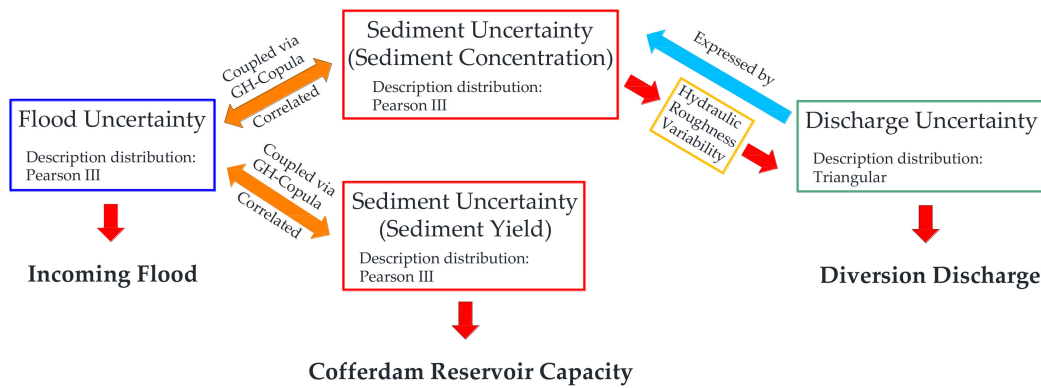

Figure 3. Relationships among the diversion uncertainties.

4. Methodology

To assess the risk of sandy river diversion during dam construction, the diversion risk definition should be determined first. Then, the appropriate method of simulation is selected, and the process of quantitative risk evaluation is presented.

4.1. Risk Definition of Dam Construction Diversion

According to ISO 31000:20009, "risk" is defined as the effect that uncertainty has on an organization's objectives [57]. For the dam construction diversion process, the delay and loss of dam construction caused by diversion works failure is the diversion risk. And flow overtopping of the upstream cofferdam is the cause of diversion failure. Therefore, the probability of upstream cofferdam overtopping can also measure the amount of construction diversion risk. In other words, the construction diversion risk can be assessed by Formula (15):

$$R = 1 - F_H(h_u) = 1 - P[H \leq h_u] \tag{15}$$

where *R* is the risk assessment result; F_H is the distribution of water levels at the upstream cofferdam, constituted by the set of all possible values of river water levels at the upstream cofferdam *H*; h_u is the crest elevation of the upstream cofferdam; and $F_H(h_u) = P[H \leq h_u]$ is the probability of water levels lower than h_u within F_H.

In actual practice, the overtopping probability is obtained by the frequency statistics of water level sampling that hits the area corresponding to cofferdam overtopping higher than h_u. Each water level value of the sampling can be generated by flood detention volume V_F, and the data of cofferdam reservoir capacity as general reservoirs all have a fixed relation between water storage volume and corresponding water levels. In this study, the flood detention volume V_F is determined by sediment-impacted diversion discharge ability q' and incoming flood process Q_{in}; the reservoir's fixed relation between water storage and water level is V'-H_u, as determined in Formula (4). Therefore, by substituting simulated samples of max flood detention volume V_F into the V'-H_u relation, the corresponding water level values can be obtained. With enough water level samples, F_H is obtained,

and h_u can serve as the variable so that an R-h_u curve can be generated, to show the relationship between the diversion risk value and corresponding crest elevation of the upstream cofferdam.

4.2. Simulation Method Selection

As the probability of upstream cofferdam overtopping corresponds to the risk value of dam construction diversion, a simulation-based sampling method can serve as the calculator. Specifically, probability can be obtained through a large sampling by statistics, and simulation can generate enough independent and credible random samples to reflect the actual risk feature.

To obtain a suitable simulation method for the risk assessment, a brief summary for existing popular risk analysis methods is necessary. Monte Carlo simulation (MCS) is a probabilistic mathematical technique used in a quantitative manner [58], and is recommended as an effective tool for risk impact analysis [59]. The first-order second-moment method (FOSM) and the point estimation method (PEM) are also popular probabilistic methods, although they are not as direct as MCS [60]. In risk analysis, the results of FOSM and MCS have close similarities [60,61] and FOSM saves computational effort [61]. However, the FOSM is limited to situations when the mean and variance can sufficiently quantify the uncertainty, rather than a full distribution; therefore, the accuracy of the FOSM for complex nonlinear problems cannot be guaranteed [62]. And PEM also has limitations, due to the need of a special, implicitly-limited state function [60]. MCS has a wider application, but the method requires proper probability distributions to describe every risk variable [59]. Since the flood and sediment uncertainties in this paper are described by the Pearson III distribution, the MCS is feasible in application. Moreover, MCS is commonly applied in construction risk management and is considered an efficient and direct method [18,19,63,64]. Hence, MCS is selected as the method of dam construction diversion simulation.

4.3. MCS-Based Dam Construction Diversion Risk Assessment

MCS generally includes generating random samples of input variables and the simulation of output results for the objective questions. In this paper, the objective of MCS is to obtain the relation curve of diversion risk and upstream cofferdam crest elevation, which is based on the distribution of water levels at the upstream cofferdam, i.e., F_H. Moreover, as water level distribution is constituted by a large number of water level values, and each MCS can output only a single water level value at a time, the MCS should be repeated over and over again until the water level distribution F_H gets enough data. The total count of MCS is set as m.

The variables of flood and sediment are needed in the simulation, and as is described in Section 3, the sample of flood peak p can be used to work out the value of both flood and sediment parameters. Hence p is the only input variable in the sampling part that can be generated through pseudo-random numbers based sampling. The method requires performing random sampling that follows the Pearson III distribution, and the key parameters of the Pearson III distribution should adopt the hydrologic observation data of the Jing River, so that the simulated data of flood peak p can best match the actual conditions in the construction site.

After the simulation, R-h_u curves can be obtained with the water level values at the upstream cofferdam. The core computational method is the water balance calculation, a common hydrology technique for determining the time and magnitude of a flood on a watercourse [65,66]. As the incoming flood process Q_{in} describes the flood near the dam site, the water balance calculation between upstream and downstream of the diversion tunnel can generate the water level at the upstream cofferdam. As Figure 4 shows, the water balance method calculates the max flood detention volume V_F by subtracting inflow volume from outflow volume within the flood cumulating period. As the flood process Q_{in} represents sequential flood traffic, which indicates the volume and timing information of a flood in a certain watershed, it can be adapted as inflow data. Meanwhile, the sediment-impacted diversion discharge ability q' can determine the outflow data. With max flood detention volume,

the upstream water level at cofferdam can be found by substituting V_F into the V'-H_u relation of Formula (4), and the water levels at the upstream cofferdam can be determined.
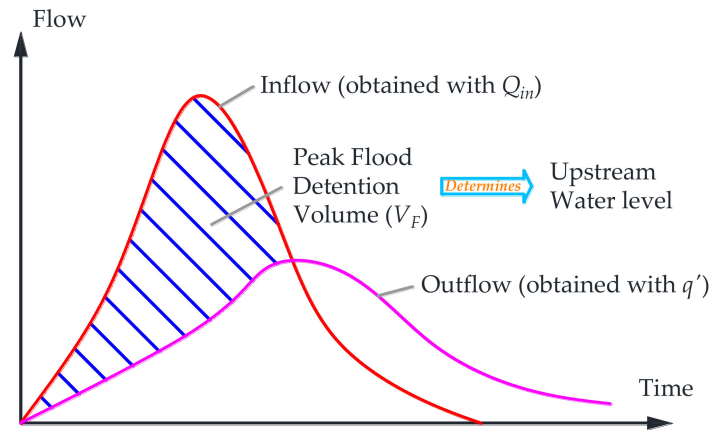
Figure 4. Rationale of flood detention assessment by water balance calculation.

For one MCS circulation, the procedure includes the calculation of reservoir capacity, discharge ability, and the determination of the incoming flood process, after which a water balance calculation can be conducted. According to Formulas (4) and (10), as well as Formulas (13) and (14), under the impact of sediment, the sediment deposition-impacted reservoir capacity V' can be obtained with the sediment variable w and the origin reservoir capacity relation of V-H_u; the sediment impacted discharge ability q' can be obtained with the sediment variable of s, the channel's water level H_d, runoff volume Q_d, and upstream waterhead H_0. As the relations of V-H_u and H_d-Q_d is known, w and s are generated by flood peak p through GH copula functions. In addition, H_u and H_0 adopt the equal value of the water level at the upstream cofferdam, so the relation of V'-H and q'-H can be obtained.

The flood process Q_{in} can be determined by flood peak p and the typical flood process of the Jing River through homogeneous proportion scaling [47]. The principle of flood process generating is that for an observed watershed, a typical flood process can be determined with measured data and based on hydrologic laws, after which floods in the watershed can be considered as being in proportion to the typical flood process. Hence, with a determinate flood peak value and the typical flood process, the flood process can be obtained.

Based on the aforementioned theoretical analysis, the function of risk assessment of dam construction diversion is shown in Formula (16).

$$\begin{cases} p_i \sim f(x)\big|_{(C_s, C_v, \bar{x})} \\ Q_{in_i} = f_{sc}(p_i) \\ w_i \sim F_{QW}^{-1}(p, w)\big|_{p_i, \theta_1} \\ s_i \sim F_{QS}^{-1}(p, s)\big|_{p_i, \theta_2} \\ V'_i = f_1(H_u, W)\big|_{W=w_i} \\ n_i = Tri(n^*)\big|_{s_i} \\ q'_i = f_2(H_0, n)\big|_{n=n_i} \\ H_i = WB(Q_{in_i}, V'_i, q'_i) \\ R = 1 - P[H \le h_u], H = \{H_i\}, i = 1, \dots, m \end{cases} \tag{16}$$

Here, $f_{sc}(p_i)$ is the homogeneous proportion scaling function for a flood with p as a variable; $WB(Q_{in_i}, V'_i, q'_i)$ is the water balance calculation function with Q_{in}, V', and q' as variables; and m is the total count of MCS.

The risk assessment process is shown in Figure 5, according to the Formula (16). With samples of flood peak p, the data of s and w can be generated through two GH copula functions, and the

hydraulic roughness coefficient *n* is determined with *s* and the triangular distribution treatment. Then, with determined V-H_u and H_d-Q_d relations, the sediment-impacted diversion parameters of q' and V' are obtained in the form of V'-H and q'-H relationships. With *p* and typical flood process, the flood process Q_{in} is determined. With q', V', and Q_{in}, a water balance calculation is conducted, and the values of the water level at the upstream cofferdam can be output. Through numerous repetitions of MCS, the distribution of water levels at the upstream cofferdam F_H can be generated through statistics, with large amount of water level samples. With F_H, the risk value curves R-h_u are generated, so that the sandy river dam construction diversion risk can be assessed.
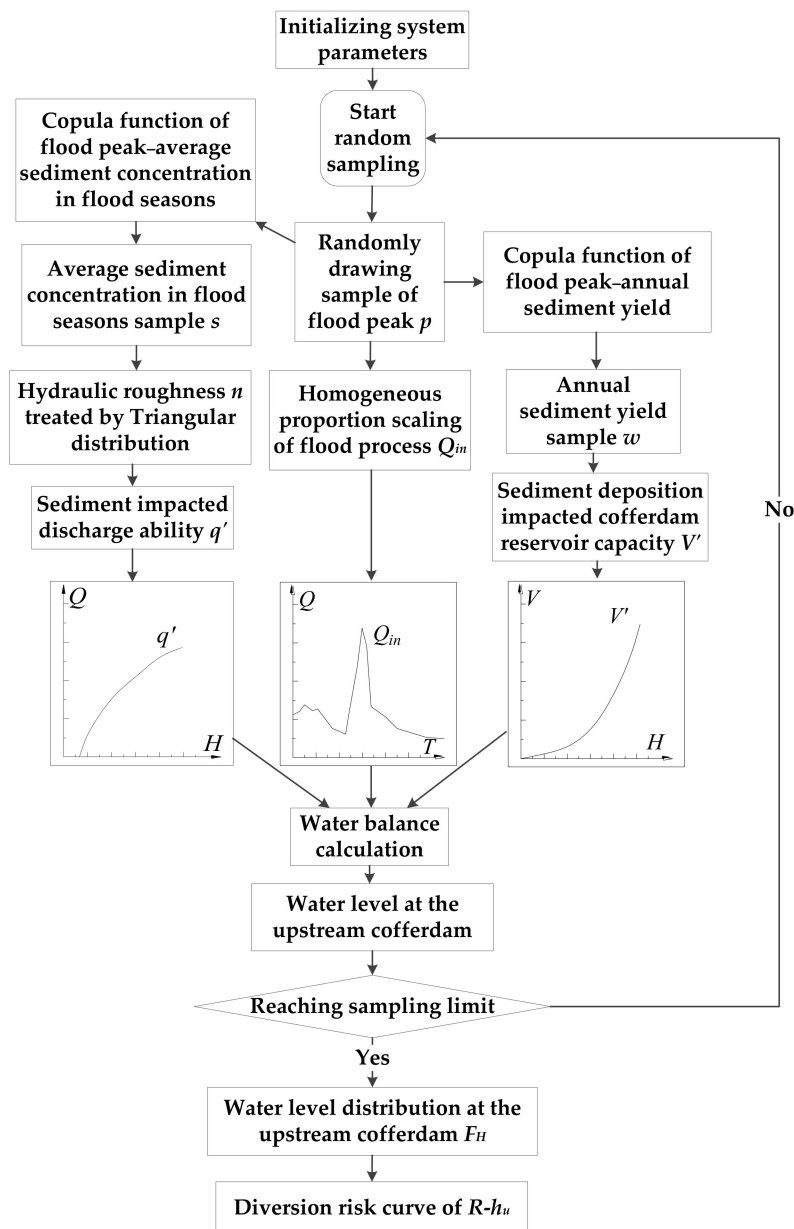

Figure 5. Schematic flow chart of generating water level distribution at the upstream cofferdam.

5. Results and Analysis

5.1. Risk Assessment Results of Dam Construction Diversion on the Jing River

To assess the risk of river diversion during dam construction on the Jing River, the required parameters involved in the aforementioned method should be provided.

As the flood and sediment all follow the Pearson III distribution, the related parameters of C_s, C_v, and $\bar{x}$ of Formula (1) should be determined so that the distribution which suits the feature of the Jing River can be obtained. Meanwhile, annual sediment yield and average sediment concentration in flood seasons is important for the coupling of sediment and flooding; therefore, the copula parameter of θ in Formula (11) should be determined as well.

Based on hydrological data between 1965 and 1988 (Tables A1 and A2) in Appendix A, the parameters of the Jing River's Pearson III distribution and copula function can be obtained in Tables 1 and 2, respectively.

Table 1. Pearson III distribution parameters of the flood and sediment series.

Series	$\bar{x}$	C_v	C_s/C_v
Flood peak volume (m³/s)	2330	1.15	3.00
Annual sediment yield (10⁴ t)	23753	0.67	2.36
Average sediment concentration in flood seasons (kg/m³)	212	0.16	11.25

Table 2. Copula function parameters of flood and sediment joint distribution.

Series of Joint Distribution	Parameters of Copula Function	
	τ	θ
Flood peak–Annual sediment yield	0.703	3.37
Flood peak–Average sediment concentration in flood seasons	0.167	1.2

The inflow and outflow data of the diversion system and the storage capacity of the cofferdam reservoir are both important for calculating the water levels in the water balance process. The diversion inflow data adapts the flood process generated by MCS and based on local typical flood process. In this paper, the typical flood course can be seen in Figure 6.
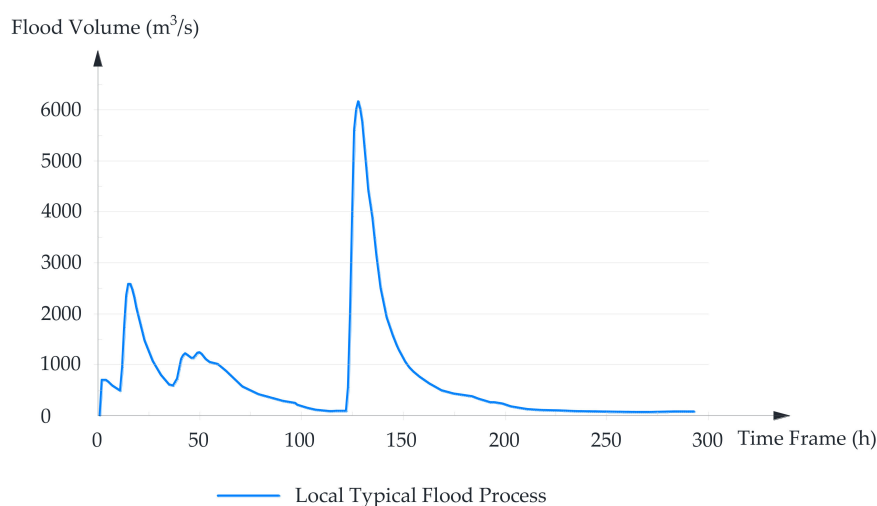

Figure 6. Typical flood process of the Jing River.

The storage parameters of the cofferdam reservoir are provided in the form of the relationship between reservoir capacity V and water level H_u, which is shown in Table A3 in Appendix A.

Meanwhile, as the Jing River's diversion project is in cofferdam and tunnel mode, the discharge ability of the diversion system is determined by the dimension of the diversion tunnel. According to the project design, one 912.44 m-long diversion tunnel with an archway profile of 17 m × 19 m,

has been adapted. The tunnel's entrance elevation is 593.00 m, its exit elevation is 589.81 m, and its gradient is 0.0035. These parameters can be seen in Table 3.

Table 3. Parameters of the diversion tunnel.

Profile Dimension (m)	Long (m) L	Area (m^3) A	Hydraulic Radius R_d	Gradient i	Sum Head Loss $\sum \zeta$
17×19	912.44	298.74	4.544	0.0035	0.9876

The roughness coefficient of the tunnel under a general clear water scenario is set as 0.014, and the relationship between the channel's water level H_d and runoff volume Q_d is in Table A4 in Appendix A.

With all the data provided, the risk of dam construction diversion on the Jing River can be assessed. To analyze the impact brought on by river sediment, the Jing River's situation and a control sample of a clear water situation are provided. For the two scenarios, the only difference lies in the sediment impact. In the Jing River sample, the sediment impact is included in the risk calculation, while in the clear water sample the sediment impact does not exist, and therefore there is no amendment of reservoir capacity and diversion discharge ability. That is, the assessment results include the dam construction diversion risk curves with sediment impact and without sediment impact.

To ensure the accuracy, MCS should be conducted enough times to collect stable results. For the clear water case, 100,000 times is enough, while for Jing River case 1 million times is needed to output a stable risk value. The result of diversion risk assessment is shown in Figure 7, in the form of two risk curves (5–20%), revealing the relationship between diversion risk value R and the corresponding safety crest elevation of the upstream cofferdam h_u, with or without sediment impact. The Jing River case's process data from GH copula and MCS computation is available in Table S1 (Supplementary Materials).
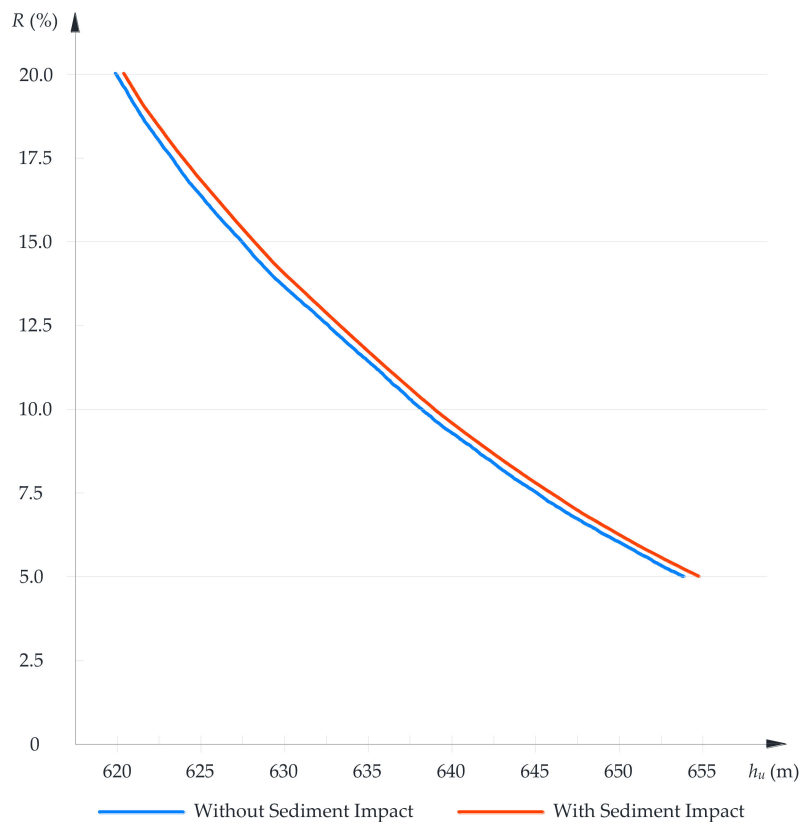

Figure 7. Dam construction diversion risk curves, with or without sediment impact (R-h_u).

5.2. Analysis of Project Case Results

The diversion system that considers sediment impact clearly needs more computations to generate stable risk results, which is explained by the rise of random dimensions. The risk origin of diversion system without sediment impact is mainly the flood factor, and the risk origin of a diversion system with sediment impact is mainly flood factors and two types of sediment factors. Hence, the random dimensions of diversion systems vary from one dimension in a clear water case to two sets of two dimensions in a sandy river case. More dimensions surely make the system more scattered. Evidently, with sediment impact, the risk assessment complexity of diversion systems increases.

The results of risk assessment show that the risk orientation of sediment impact is negative. According to Figure 7, it is evident that with the impact of sediment, the risk value of river diversion during dam construction is higher, under the same crest elevation. To fully illustrate the risk feature, four representative risk values of 5%, 10%, 15%, and 20%, along with corresponding safety cofferdam crest elevations of the Jing River case and clear water case contrast are provided in Table 4. The crest difference of the two cases are also included.

Table 4. Four risk values and corresponding safety crest elevations of the Jing River case and clear water contrast, as well as crest difference.

Jing River Case		Contrast Clear Water Case		Crest Difference Considering Sediment Impact (m)
Risk Value R (%)	Corresponding Safety Crest of Cofferdam h_u (m)	Risk Value R (%)	Corresponding Safety Crest of Cofferdam h_u (m)	
5	654.72	5	653.86	+0.86
10	638.94	10	638.15	+0.79
15	628.14	15	627.44	+0.70
20	620.34	20	619.92	+0.42

As is shown in Table 4, with sediment impact, the corresponding safety cofferdam crest elevation rise varies from 0.42 m to 0.86 m. The degree of elevation rise increases with the elevation of the diversion assurance, i.e., safer diversion plans need to further heighten the cofferdam. For example, the diversion systems that have the high assurance rate of 95% (risk value at 5%) and 90% (risk value at 10%) all see an evident increase of 0.86 m and 0.79 m, respectively, in corresponding safety upstream cofferdam crest elevations after considering the sediment impact; however, for more economical diversion schemes, like the 80% assurance case (risk value at 20%), the cofferdam crest increase contributed by sediment impacts is just 0.42 m. Based on hydrology, flooding with a higher flood peak is generally less possible. Therefore, by heightening the cofferdams, the diversion system can resist a larger flood and possesses higher assurance. Hence, from the risk results, it can be concluded that sediment impact is relatively evident in safer plans, which have a higher assurance.

The elevation of the cofferdam crest counteracts negative influences, like cofferdam reservoir capacity shrinkage and the reduction of discharge ability, which is related to sediment yield and sediment concentration. As the risk feature of diversion system shows that sediment impact increases with the rise of diversion assurance, the correlation between flood and sediment is proved and reflected. Specifically, higher assurance means that the diversion systems need to resist larger scales of possible flooding, which have a higher flood peak. Based on the coupling of flood and sediment (described in Section 3.5), a higher flood peak volume brought more sediment into the river flow, which increases the annual sediment yield and sediment concentration. With a higher annual sediment yield, the reservoir deposition surely becomes more serious, which occupies the capacity for flood detention and makes the water level at the cofferdam higher. Meanwhile, the change of sediment concentration influences the discharge ability of a diversion system, which is mostly bad for diversion. Hence, the degradation brought on by sediment impact increases with the increase of flood-resisting standards.

6. Conclusions

This paper proposes a simulation-based risk assessment method for river diversion during dam construction under sediment impact, and only discusses the river cut-off cofferdam and tunnel diversion mode. With this method, the sediment impact on diversion risk is assessed by introducing a dam construction diversion project on the Jing River, one of the sandy rivers in China, together with a clear water version for contrast.

Diversion risk derives from uncertainties, and is assessed by the probability of an upstream cofferdam overtopping during flood. To obtain the probability of overtopping, diversion uncertainties of flood and sediment were analyzed. Sediment uncertainty was divided into two types, as sediment yield influences diversion storage, while sediment concentration influences diversion discharge through variability in hydraulic roughness. Meanwhile, as flood and sediment uncertainties are correlated, one GH copula function was introduced, to couple the flood peak and sediment yield, and another GH copula function was utilized for the flood peak and sediment concentrations. With the two flood–sediment GH copula functions, the parameters of the diversion system storage and discharge, as well as flooding, can be generated based on simulation. Hence, the MCS, together with the water balance calculation, was adopted to simulate the operation of the diversion system and output the water level values at the upstream cofferdam. Finally, through the frequency statistics of water level values, the cofferdam overtopping probability could be obtained, i.e., the dam construction diversion risk could be assessed.

In actual practice, the simulation-based method can quantitatively assess the risk of the Jing River diversion project, as well as the clear water contrast. The risk results output by the method are stable and can reflect certain risk features. From the results of the risk assessment, it can be concluded that for dam construction diversion on sandy rivers, sediment impact should be paid attention to, for it has a negative influence on diversion risk. Diversion risk value rises when considering sediment impact, therefore a higher cofferdam should be adopted to maintain the same risk. The degree of sediment impact is also related to diversion assurance, in that higher diversion assurance schemes suffer greater impact from sediment. Hence, diversion systems on sandy rivers need more of an effort with relation to risk management than generally clear water rivers.

Author Contributions: Quan Liu, Zhigen Hu and Zida Song conceived and designed the method; Quan Liu and Zida Song performed the computation and analyzed the data; Huian Li and Jianqing Xiong contributed project data and key parameters; Zida Song and Quan Liu wrote the paper.

Conflicts of Interest: The authors declare no conflict of interest.

Appendix A

Table A1. Measured data of annual precipitation and annual sediment yield (Jing River).

Year	Annual Precipitation (10^8 m^3)	Annual Sedimen Yield (10^4 t)	Year	Annual Precipitation (10^8 m^3)	Annual Sediment Yield (10^4 t)
1965	14.12	5644	1977	17.60	42,800
1966	31.65	63,557	1978	17.00	25,200
1967	21.33	13,293	1979	11.90	16,200
1968	26.56	32,760	1980	13.60	16,700
1969	15.97	21,700	1981	21.90	23,500

Table A1. Cont.

Year	Annual Precipitation (10^8 m^3)	Annual Sedimen Yield (10^4 t)	Year	Annual Precipitation (10^8 m^3)	Annual Sediment Yield (10^4 t)
1970	24.15	41,900	1982	13.10	12,800
1971	12.99	15,900	1983	22.90	11,700
1972	8.47	4150	1984	23.00	27,000
1973	21.06	52,600	1985	18.50	19,200
1974	13.25	15,300	1986	11.60	10,500
1975	26.05	25,600	1987	9.32	9190
1976	21.93	19,900	1988	22.20	43,000

Table A2. Measured data of flood peak volume and average sediment concentration in flood seasons (Jing River).

Year	Flood Peak Volume (m^3/s)	Average Sediment Concentration in Flood Seasons (kg/m^3)	Year	Flood Peak Volume (m^3/s)	Average Sediment Concentration in Flood Seasons (kg/m^3)
1965	507	191	1977	1870	242
1966	7520	192	1978	1520	178
1967	950	209	1979	1060	200
1968	1480	230	1980	1100	194
1969	1110	199	1981	1630	242
1970	2700	224	1982	927	195
1971	1410	222	1983	833	168
1972	398	192	1984	1350	205
1973	6160	214	1985	610	203
1974	866	215	1986	1760	212
1975	2390	160	1987	662	213
1976	1180	196	1988	1960	193

Table A3. Relationship between origin reservoir capacity V and reservoir water level H_u.

Water Level (m)	Origin Reservoir Capacity (10^4 m^3)	Water Level (m)	Origin Reservoir Capacity (10^4 m^3)	Water Level (m)	Origin Reservoir Capacity (10^4 m^3)
586.69	0	612	158	638	2354
588	0.1	614	204	640	2712
590	1	616	262	642	3113
592	2	618	344	644	3550
594	3	620	440	646	4026
596	5	622	555	648	4545
598	10	624	696	650	5111
600	17	626	857	652	5717
602	26	628	1040	654	6357
604	42	630	1246	656	7032
606	64	632	1477	658	7747
608	89	634	1740	660	8521
610	119	636	2032		

Table A4. Relationship between channel's water level H_d and runoff volume Q_d.

Water Level H_d (m)	Runoff Volume Q_d (m^3/s)	Water Level H_d (m)	Runoff Volume Q_d (m^3/s)	Water Level H_d (m)	Runoff Volume Q_d (m^3/s)
586.59	0	605.88	2600	616.12	6200
587.45	25	606.66	2800	616.96	6600
588.26	50	607.39	3000	617.77	7000
589.21	100	608.09	3200	618.56	7400
590.77	200	608.79	3400	619.32	7800

Table A4. Cont.

Water Level H_d (m)	Runoff Volume Q_d (m³/s)	Water Level H_d (m)	Runoff Volume Q_d (m³/s)	Water Level H_d (m)	Runoff Volume Q_d (m³/s)
592.16	300	609.47	3600	620.06	8200
594.27	500	610.13	3800	620.77	8600
596.00	700	610.77	4000	621.46	9000
598.15	1000	611.38	4200	622.28	9500
599.60	1250	611.96	4400	623.06	10,000
601.46	1600	612.51	4600	626.08	12,000
602.44	1800	613.03	4800	627.56	13,000
603.35	2000	613.50	5000	629.03	14,000
604.22	2200	614.40	5400	630.45	15,000
605.06	2400	615.27	5800	637.38	20,000

Notation List

A	cross-section area of the discharge tunnel
α, β, a_0	distribution parameters of the Pearson III distribution
C_d	Chézy coefficient
C_s	coefficient of deviation
C_v	coefficient of variation
C_k^2	combinatorial number of 2 variables with a length of k
e	Napier constant
F_H	distribution of water levels at the upstream cofferdam
$F_Q(p)$	marginal distribution functions of flood peak
$F_S(s)$	marginal distribution functions of average sediment concentration in flood seasons
$F_W(w)$	marginal distribution functions of annual sediment yield
$F_Y(y)$	marginal distribution function of flood peak variable y
$F_Z(z)$	marginal distribution function of sediment variables z
$f_{sc}(p_i)$	homogeneous proportion scaling function with p as the variable.
g	gravitational acceleration
H	set of all possible values of river water levels at the upstream cofferdam
H_d	river channel's water level
H_u	upstream cofferdam reservoir water level
H_0	upstream waterhead
h_p	difference of downstream water level and the downstream diversion tunnel exit elevation
h_u	crest elevation of the upstream cofferdam
i	gradient of the diversion tunnel
k_s	side wall protrude height of the diversion tunnel
L	length of the diversion tunnel
m	total sampling count of MCS
n	synthesis roughness coefficient of the diversion tunnel
n^*	value of calculated roughness that only considers sediment influence
p	sample value of flood peak volume
Q_d	river runoff volume
Q_{in}	flood process
q	capacity of diversion discharge flow
q'	sediment impacted discharge ability of the diversion tunnel
R	diversion risk assessment result
R_d	hydraulic radius of the diversion tunnel
r_s	dry bulk density of silt
S	flow average sediment concentration in flood seasons
S_v	volume sediment concentration, $S_v = S/r_s$
s	sample value of the average sediment concentration in flood seasons S

$sign(\cdot)$	sign function
T	duration of deposition (in years)
$Tri()$	Triangular distribution treatment function
V	origin upstream cofferdam reservoir capacity
V'	sediment deposition impacted upstream cofferdam reservoir capacity
V_F	max flood detention volume
V_s	reservoir sediment deposition volume
W	annual sediment yield
$WB(Q_{in_i}, V'_i, q'_i)$	water balance calculation function with Q_{in}, V', q' as variables
w	sample value of annual sediment yield W
x	value of random variables that obey Pearson III distribution
$\bar{x}$	mean value of random variables that obey Pearson III distribution
(y_i, z_i)	sample data of flood peak and sediment variables
$\Gamma(\alpha)$	Gamma function of the Pearson III distribution parameter α
δ	deposit rate determined based on regional hydrology and sediment data
η	ratio of the bed load among the suspended load
θ	parameter of GH-copula function
κ	Karman constant
μ	discharge coefficient of the diversion tunnel
τ	Kendall correlation coefficient
ϕ	sediment porosity
χ	correction coefficient for Formula (8)
$\sum \zeta$	sum of waterhead loss of the diversion tunnel

References

1. International Commission on Large Dams. WORLD REGISTER OF DAMS/General Synthesis. Available online: http://www.icold-cigb.org/GB/world_register/general_synthesis.asp (accessed on 19 November 2017).

2. Hong, X.; Guo, S.; Wang, L.; Yang, G.; Liu, D.; Guo, H.; Wang, J. Evaluating water supply risk in the middle and lower reaches of Hanjiang River Basin based on an integrated optimal water resources allocation model. *Water* **2016**, *8*, 364. [CrossRef]

3. Farfan, J.; Breyer, C. Structural changes of global power generation capacity towards sustainability and the risk of stranded investments supported by a sustainability indicator. *J. Clean. Prod.* **2017**, *141*, 370–384. [CrossRef]

4. Bartle, A. Hydropower potential and development activities. *Energy Policy* **2002**, *30*, 1231–1239. [CrossRef]

5. Chang, X.L.; Liu, X.; Zhou, W. Hydropower in China at present and its further development. *Energy* **2010**, *35*, 4400–4406. [CrossRef]

6. Biemans, H.; Haddeland, I.; Kabat, P.; Ludwig, F.; Hutjes, R.W.A.; Heinke, J.; Von Bloh, W.; Gerten, D. Impact of reservoirs on river discharge and irrigation water supply during the 20th century. *Water Resour. Res.* **2011**, *47*, 1–15. [CrossRef]

7. Zarfl, C.; Lumsdon, A.E.; Berlekamp, J.; Tydecks, L.; Tockner, K. A global boom in hydropower dam construction. *Aquat. Sci.* **2014**, *77*, 161–170. [CrossRef]

8. Silveira, A. Some considerations on the durability of dams. *Water Power Dam Constr.* **1990**, *42*, 19–24.

9. Rasekh, A.; Afshar, A.; Afshar, M.H. Risk-cost optimization of hydraulic structures: Methodology and case study. *Water Resour. Manag.* **2010**, *24*, 2833–2851. [CrossRef]

10. Marengo, H.; Arreguin, F.I.; Aldama, A.A.; Morales, V. Case study: Risk analysis by overtopping of diversion works during dam construction: The La Yesca hydroelectric project, Mexico. *Struct. Saf.* **2013**, *42*, 26–34. [CrossRef]

11. Parker, T.C.; Froste, B.; McConnell, M.J. Mrica hydroelectric project civil engineering construction. *Proc. Inst. Civ. Eng.-Water Marit. Energy* **1993**, *101*, 157–172. [CrossRef]

12. Afshar, A.; Barkhordary, A.; Marino, M.A. Optimizing river diversion under hydraulic and hydrologic uncertainties. *J. Water Resour. Plan. Manag.* **1994**, *120*, 36–47. [CrossRef]

13. Dai, H.; Cao, G.; Su, H. Management and construction of the Three Gorges project. *J. Constr. Eng. Manag.* **2006**, *132*, 615–619. [CrossRef]

14. Sedighizadeh, S.; Mansoori, A.; Pirestani, M.R.; Sedighizadeh, D. A new model for economic optimization of water diversion system during dam construction using PSO algorithm. *World Acad. Sci. Eng. Technol.* **2011**, *5*, 35–41.

15. Karamouz, M.; Doroudi, S.; Ahmadi, A.; Moridi, A. Optimal design of water diversion system: A case study. In Proceedings of the World Environmental and Water Resources Congress 2009—World Environmental and Water Resources Congress 2009: Great Rivers, Kansas City, MO, USA, 17–21 May 2009.

16. Marengo, H. Case study: Dam safety during construction, lessons of the overtopping diversion works at Aguamilpa Dam. *J. Hydraul. Eng.* **2006**, *132*, 1121–1127. [CrossRef]

17. Afshar, A.; Rasekh, A.; Afshar, M.H. Risk-based optimization of large flood-diversion systems using genetic algorithms. *Eng. Optim.* **2009**, *41*, 259–273. [CrossRef]

18. Hu, Z.G.; Fan, X.E.; Liu, Q.; Huang, H. Design of integrated risk distribution mechanism of construction diversion system. *J. Hydraul. Eng.* **2006**, *37*, 1270–1277. [CrossRef]

19. Liu, Q.; Hu, Z.; Qi, Z.; Min, R. Risk feature analysis of river diversion for dam reconstruction on the original site. *Adv. Eng. Sci.* **2007**, *49*, 35–41. [CrossRef]

20. Bai, Y.; Xu, H. Hydrodynamic instability of hyperconcentrated flows of the Yellow River. *J. Hydraul. Res.* **2010**, *48*, 742–753. [CrossRef]

21. Shrestha, B.; Cochrane, T.A.; Caruso, B.S.; Arias, M.E.; Piman, T. Uncertainty in flow and sediment projections due to future climate scenarios for the 3S Rivers in the Mekong Basin. *J. Hydrol.* **2016**, *540*, 1088–1104. [CrossRef]

22. Oh, J.; Tsai, C.W.; Choi, S.-U. Quantifying the uncertainty associated with estimating sediment concentrations in open channel flows using the stochastic particle tracking method. *J. Hydraul. Eng.* **2015**, *141*. [CrossRef]

23. Rosen, T.; Xu, Y.J. A hydrograph-based sediment availability assessment: Implications for Mississippi River sediment diversion. *Water* **2014**, *6*, 564–583. [CrossRef]

24. Schmelter, M.L.; Erwin, S.O.; Wilcock, P.R. Accounting for uncertainty in cumulative sediment transport using Bayesian statistics. *Geomorphology* **2012**, *175*, 1–13. [CrossRef]

25. He, L.; Duan, J.G.; Wang, G.; Fu, X. Numerical simulation of unsteady hyperconcentrated sediment-laden flow in the Yellow River. *J. Hydraul. Eng.* **2012**, *138*, 958–969. [CrossRef]

26. Billi, P.; El Badri Ali, O. Sediment transport of the Blue Nile at Khartoum. *Quat. Int.* **2010**, *226*, 12–22. [CrossRef]

27. United States Department of the Interior Bureau of Reclamation. *Design of Small Dams*, 3rd ed.; Water Resources Technical Publications: Washington, DC, USA, 1987; ISBN -10:016003373X.

28. Kmusser. The Jing Flows into the Wei Near Xi'an. Available online: https://en.wikipedia.org/wiki/Jing_River#/media/File:Weirivermap.png (accessed on 19 November 2017).

29. Tung, Y.K.; Yen, B.C.; Melching, C.S. *Hydrosystems Engineering Reliability Assessment and Risk Analysis*; McGraw-Hill: New York, NY, USA, 2006; ISBN 0-07-145158-7.

30. Bobée, B.; Rasmussen, P.F. Recent advances in flood frequency analysis. *Rev. Geophys.* **1995**, *33*, 1111–1116. [CrossRef]

31. Vogel, R.W.; McMartin, D.E. Probability plot goodness-of-fit and skewness estimation procedures for the Pearson type 3 distribution. *Water Resour. Res.* **1991**, *27*, 3149–3158. [CrossRef]

32. Ministry of Water Resources of the People's Republic of China. *SL 303-2017 Specifications for Construction Planning of Water Resources and Hydropower Projects*; Water & Power Press: Beijing, China, 2017; ISBN 155170318. (In Chinese)

33. Wang, C.; Wang, Z. Uncertainty Analysis and Application of Construction Diversion Tunnel Discharge Capacity. In Proceedings of the 2014 International Conference on Mechatronics, Electronic, Industrial and Control Engineering (MEIC), Shenyang, China, 15–17 November 2014.

34. Nakhaei, N.; Etemad-Shahidi, A. Applying Monte Carlo and classification tree sensitivity analysis to the Zayandehrood River. *J. Hydroinform.* **2012**, *14*, 236. [CrossRef]

35. Lee, H.-Y.; Lin, Y.-T.; Yunyou, J.; Wenwang, H. On three-dimensional continuous saltating process of sediment particles near the channel bed. *J. Hydraul. Res.* **2006**, *44*, 374–389. [CrossRef]

36. Li, X.; Wei, X. Analysis of the relationship between soil erosion risk and surplus floodwater during flood season. *J. Hydrol. Eng.* **2014**, *19*, 1294–1311. [CrossRef]

37. Jin, X.; Hao, Z.; Zhang, J. Study on the relation of frequency between flood and sediment in the Middle Yellow River. *J. Sediment. Res.* **2006**, *3*, 6–13. [CrossRef]

38. Radice, A.; Longoni, L.; Papini, M.; Brambilla, D.; Ivanov, V.I. Generation of a design flood-event scenario for a mountain river with intense sediment transport. *Water* **2016**, *8*. [CrossRef]

39. Peng, Y.; Ji, C.; Gu, R. A multi-objective optimization model for coordinated regulation of flow and sediment in cascade reservoirs. *Water Resour. Manag.* **2014**, *28*, 4019–4033. [CrossRef]

40. Schleiss, A.J.; Franca, M.J.; Juez, C.; De Cesare, G. Reservoir sedimentation. *J. Hydraul. Res.* **2016**, *54*, 595–614. [CrossRef]

41. Meyer-Peter, E.; Müller, R. Formulas for Bed-Load Transport. In Proceedings of the IAHSR 2nd Meeting, Stockholm, Sweden, 7–9 June 1948; pp. 39–64.

42. Yang, C.T.; Wan, S. Comparisons of selected bed-material load formulas. *J. Hydraul. Eng.* **1991**, *117*, 973–989. [CrossRef]

43. Van den Berg, J.H.; van Gelder, A. Prediction of suspended bed material transport in flows over silt and very fine sand. *Water Resour. Res.* **1993**, *29*, 1393–1404. [CrossRef]

44. Papalaskaris, T.; Dimitriadou, P.; Hrissanthou, V. Comparison between computations and measurements of bed load transport rate in Nestos River, Greece. *Procedia Eng.* **2016**, *162*, 172–180. [CrossRef]

45. Gic-Grusza, G.; Dudkowska, A. Numerical modeling of hydrodynamics and sediment transport—An integrated approach. *Ocean Dyn.* **2017**, *67*, 1283–1292. [CrossRef]

46. Dysarz, T.; Szalkiewicz, E.; Wicher-Dysarz, J. Long-term impact of sediment deposition and erosion on water surface profiles in the Ner River. *Water* **2017**, *9*. [CrossRef]

47. Luo, W.S.; Song, X.Y. *Engineering Hydrology and Hydraulic Calculation*, 2nd ed.; Water&Power Press: Beijing, China, 2010; (In Chinese). ISBN 9787508474458.

48. Ministry of Water Resources of the People's Republic of China. *SL 623-2013 Design Code for Construction Diversion of Water Resources and Hydropower Engineering*; Water&Power Press: Beijing, China, 2013; (In Chinese). ISBN 155170.

49. Manning, R. On the Flow of Water in Open Channels and Pipes. *Trans. Inst. Civ. Eng. Irel.* **1891**, *20*, 161–207.

50. Shu, A.; Liu, Q.; Fei, X. Unified laws of velocity distribution for sediment laden flow with high and low concentration. *J. Hydraul. Eng.* **2006**, *37*, 1175–1180. [CrossRef]

51. Deng, A. Study on Key Technical Problems in Modeling of Hyper-Concentrated Flows. Master's Thesis, China Institute of Water Resources and Hydropower Research, Beijing, China, April 2007. (In Chinese)

52. Zhang, H. Vertical distribution of velocity in sediment-laden flow. *J. Sediment. Res.* **1995**, *2*, 1–10. [CrossRef]

53. Xiao, Y.; Guo, S.L.; Xiong, L.H.; Liu, P.; Fang, B. A new Random Simulation method for constructing synthetic flood hydrographs. *J. Sichuan Univ. (Eng. Sci. Ed.)* **2007**, *39*, 55–60. [CrossRef]

54. Guo, A.; Chang, J.; Wang, Y.; Huang, Q. Variations in the runoff-sediment relationship of the Weihe River Basin based on the Copula function. *Water* **2016**, *8*. [CrossRef]

55. Xu, Y.; Huang, G.; Fan, Y. Multivariate flood risk analysis for Wei River. *Stoch. Environ. Res. Risk Assess.* **2017**, *31*, 225–242. [CrossRef]

56. Nelsen, R.B. *An Introduction to Copulas*, 2nd ed.; Springer: New York, NY, USA, 2006; ISBN 978-0-387-28659-4.

57. International Organization for Standardization (ISO). *ISO 31000:2009 Risk Management—Principles and Guidelines*; ISO: Geneva, Switzerland, 2009; ISBN 0733792898.

58. Elbarkouky, M.M.G.; Fayek, A.R.; Siraj, N.B.; Sadeghi, N. Fuzzy arithmetic risk analysis approach to determine construction project contingency. *J. Constr. Eng. Manag.* **2016**, *142*, 4016070. [CrossRef]

59. Chang, C.; Ko, J. New approach to estimating the standard deviations of lognormal cost variables in the Monte Carlo analysis of construction risks. *J. Constr. Eng. Manag.* **2016**, 1–7. [CrossRef]

60. Adarsh, S.; Reddy, M.J. Reliability analysis of composite channels using first order approximation and Monte Carlo simulations. *Stoch. Environ. Res. Risk Assess.* **2013**, *27*, 477–487. [CrossRef]

61. Ganji, A.; Jowkarshorijeh, L. Advance first order second moment (AFOSM) method for single reservoir operation reliability analysis: A case study. *Stoch. Environ. Res. Risk Assess.* **2012**, *26*, 33–42. [CrossRef]

62. Mishra, S. Uncertainty and sensitivity analysis techniques for hydrologic modeling. *J. Hydroinform.* **2009**, *11*, 282. [CrossRef]

63. Sadeghi, N.; Fayek, A.R.; Pedrycz, W. Fuzzy Monte Carlo simulation and risk assessment in construction. *Comput. Civ. Infrastruct. Eng.* **2010**, *25*, 238–252. [CrossRef]

64. Rohaninejad, M.; Bagherpour, M. Application of risk analysis within value management: A case study in dam engineering. *J. Civ. Eng. Manag.* **2013**, *19*, 364–374. [CrossRef]

65. Chow, V.T.; Maidment, D.R.; Mays, L.W. *Applied Hydrology*; McGraw-Hill: Singapore, 1988; ISBN 9780071001748.
66. Li, B.; Liang, Z.; Zhang, J.; Chen, X.; Jiang, X.; Wang, J.; Hu, Y. Risk analysis of reservoir flood routing calculation based on inflow forecast uncertainty. *Water* **2016**, *8*, 486. [CrossRef]